Life Sciences 84 (2009) 499–504

Contents lists available at ScienceDirect

Life Sciences

journal homepage: www.elsevier.com/locate/lifescie

TNF-α and IL-1β inhibit RUNX2 and collagen expression but increase alkaline phosphatase activity and mineralization in human mesenchymal stem cells

J. Ding [a,b], O. Ghali [a], P. Lencel [a], O. Broux [a], C. Chauveau [a], J.C. Devedjian [a], P. Hardouin [a], D. Magne [a,*]

[a] Laboratory of Cellular and Molecular Biology EA2603, IFR114, ULCO, Université Lille Nord de France, France
[b] Department of Orthopaedic surgery, Shanghai Jiaotong University Affiliated Sixth People's Hospital, Shanghai, China

ARTICLE INFO

Article history:
Received 10 July 2008
Accepted 23 January 2009

Keywords:
TNF-α
IL-1β
MSC
Bone formation
Spondyloarthropathy

ABSTRACT

Aims: Joint inflammation leads to bone erosion in rheumatoid arthritis (RA), whereas it induces new bone formation in spondyloarthropathies (SpAs). Our aims were to clarify the effects of tumour necrosis factor α (TNF-α) and interleukin 1β (IL-1β) on osteoblast differentiation and mineralization in human mesenchymal stem cells (MSCs).
Main methods: In MSCs, expression of osteoblast markers was assessed by real-time PCR and ELISA. Activity of tissue-nonspecific alkaline phosphatase (TNAP) and mineralization were determined by the method of Lowry and alizarin red staining respectively. Involvement of RUNX2 in cytokine effects was investigated in osteoblast-like cells transfected with a dominant negative construct.
Key findings: TNF-α (from 0.1 to 10 ng/ml) and IL-1β (from 0.1 to 1 ng/ml) stimulated TNAP activity and mineralization in MSCs. Addition of 50 ng/ml of IL-1 receptor antagonist in TNF-α-treated cultures did not reverse TNF-α effects, indicating that IL-1 was not involved in TNF-α-stimulated TNAP activity. Both TNF-α and IL-1β decreased *RUNX2* expression and osteocalcin secretion, suggesting that RUNX2 was not involved in mineralization. This hypothesis was confirmed in osteoblast-like cells expressing a dominant negative RUNX2, in which TNAP expression and activity were not reduced. Finally, since mineralization may merely rely on increased TNAP activity in a collagen-rich tissue, we investigated cytokine effects on collagen expression, and observed that cytokines decreased collagen expression in osteoblasts from MSC cultures.
Significance: The different effects of cytokines on TNAP activity and collagen expression may therefore help explain why inflammation decreases bone formation in RA whereas it induces ectopic ossification from collagen-rich entheses during SpAs.

Introduction

Tumor necrosis factor (TNF)-α and interleukin (IL)-1β are two major cytokines that lead to bone loss in many inflammatory diseases. In rheumatoid arthritis (RA) for instance, bone loss is reduced by therapies blocking TNF-α or IL-1β [for review see (Walsh et al. 2005)]. Interfering with TNF-α and IL-1β action may also be beneficial in preventing bone loss in diseases not usually considered as inflammatory, such as post-menopausal osteoporosis. Indeed, ovariectomized mice do not lose bone in absence of TNF-α (Ammann et al. 1997; Kimble et al. 1997) or IL-1 (Kimble et al. 1995; Kitazawa et al. 1994; Lorenzo et al. 1998). Moreover, bone resorption due to estrogen deficiency in women may be blocked by etanercept and anakinra, which are inhibitors of TNF-α or IL-1β respectively (Charatcharoenwitthaya et al. 2007).

The mechanisms used by TNF-α and IL-1β to promote bone loss include activation of osteoclastogenesis, which occurs both directly (Jimi et al. 1999; Kitaura et al. 2004) and also through the expression by stromal cells of receptor activator of nuclear factor κB ligand (RANKL) and macrophage colony stimulating factor (MCSF) (Kitaura et al. 2005; Wei et al. 2005). It is also generally recognized that both cytokines contribute to decrease bone mineral density by inhibiting osteoblast differentiation and bone formation. TNF-α for instance has been reported to decrease RUNX2 expression (Gilbert et al. 2002) and promote its degradation (Kaneki et al. 2006).

In contrast to their effects on bone loss, inflammatory cytokines are strongly suspected to induce ectopic bone formation, for instance in arteries during atherosclerosis and type II diabetes, or during aortic valve disease (Demer 2002; Doherty et al. 2003; Helske et al. 2007). For instance, a recent article importantly reported that in *ldlr*-/- diabetic mice, inflammation and aortic calcification are reduced upon treatment with the TNF-α inhibitor infliximab, whereas weight gain, hyperglycemia, hypercholesterolemia, or hyperleptinemia remain unaffected (Al-Aly et al. 2007). Underlying mechanisms may involve the reported positive effects of TNF-α and IL-1β on tissue-nonspecific

* Corresponding author. Laboratory of Cellular and Molecular Biology, Quai Masset, Bassin Napoléon BP120, 62327 Boulogne sur mer, France. Tel.: +33 3 21 99 45 22; fax: +33 3 21 99 45 24.
E-mail address: david.magne@univ-littoral.fr (D. Magne).

0024-3205/$ – see front matter © 2009 Elsevier Inc. All rights reserved.
doi:10.1016/j.lfs.2009.01.013

alkaline phosphatase (TNAP) expression by vascular smooth muscle cells (VSMCs) (Parhami et al. 2002; Shioi et al. 2002; Tintut et al. 2000, 2002) and myofibroblasts (Al-Aly et al. 2007; Kaden et al. 2005).

Inflammatory vascular calcification, as well as inflammatory bone loss, may have dramatic consequences [reviewed in (Doherty et al. 2003; Shao et al. 2006)]. A better understanding of the effects of inflammatory mediators on new bone formation in normal and ectopic sites is therefore warranted. In this context, aims of the study reported here were to determine TNF-α and IL-1β effects on osteoblast differentiation and mineralization in human mesenchymal stem cells (MSCs), which are osteoblast and VSMC precursors [reviewed in (Magne et al. 2005)]. In addition, our goal was also to investigate whether TNF-α effects on osteoblast differentiation and mineralization may depend on IL-1, since RANKL secretion induced by TNF-α in stromal cells requires the presence of IL-1 signaling (Wei et al. 2005).

Materials and methods

Chemicals

Cell culture plastic ware was purchased from D. Dutscher (Brumath, France). Dulbecco's minimum essential medium (DMEM), α-MEM, fetal calf serum (FCS), L-glutamine, penicillin, streptomycin (P/S), trypsin/EDTA, and Extract-All reagents were from Eurobio (Les Ulis, France). Vitamin D3 (VD3), vitamin C, β-glycerophosphate (β-GP), p-nitrophenylphosphate, cetyl pyridinium chloride were obtained from Sigma-Aldrich Corporation (St Quentin Fallavier, France). DNase I, Taq DNA polymerase and SYBR green mix were from Roche Diagnostic (Meylan, France). Random primers were obtained from TibMolBiol (Berlin, Germany). Superscript II reverse transcriptase and dNTPs were purchased from Invitrogen (Cergy Pontoise, France). TNF-α, IL-1β and IL-1 receptor antagonist (IL-1Ra) were purchased from R&D Systems (Lille, France).

Cell culture

To investigate osteoblast differentiation, cells from four patients were used. Cells consisted in purified MSCs from a healthy 34-year-old female (Cambrex Bio Science, Walkersville, USA; certified positive for CD29, CD44, CD105 and CD166, and negative for CD14, CD34 and CD45) and also in bone marrow stromal cells obtained from trabecular bone explants prepared from the iliac crest bone harvested during pelvic osteotomy in three other patients (from 2.5 to 10 years-old) with Legg–Perthes–Calve disease. According to our regional ethic committee, surgeons asked informed consent to the children's parents. Legg–Perthes–Calve disease is an idiopathic avascular necrosis of the femoral head, which does not affect the iliac crest. Bone marrow was extracted as previously published in details (Anselme et al. 2000). Briefly, a small part of the body iliac crest was removed at the end of the surgery in order to close without creating tension of the iliac crest. This fragment of bone was sent to the laboratory, where it was minced into small pieces, and extensively washed with PBS to obtain the bone marrow cells. Cells were isolated by centrifugation, and stromal cells were separated from non-adherent cells by several washes in culture. Purified MSCs or MSCs in bone marrow stromal cells were seeded at a density of 5000 cells/cm^2 and routinely cultured in DMEM containing 10% FCS, 1% P/S, and 1% L-glutamine. Cells were maintained at 37 °C in a humidified atmosphere with 5% CO_2 in air. Cells were subcultured at approximately 80–90% confluence with trypsin/EDTA. Osteoblastic differentiation was induced by culturing cells in an osteogenic medium, containing 10^{-8} M VD3, 50 μM vitamin C and 10 mM β-GP, as previously reported (Isaac et al. 2008). Media were changed every 2 or 3 days. To investigate the effects of cytokines, cells were treated from day 2 with TNF-α (0.1 to 10 ng/ml) and/or IL-1β (0.1 to 1 ng/ml) and cytokines were added in the medium at each change. To assess the effects of IL-1Ra, new medium with IL-1Ra was changed 2 h before addition of TNF-α and/or IL-1β.

To investigate whether cytokine effects were dependent on RUNX2, human SaOS-2 osteoblast-like cells were transfected with a construct encoding the RUNX2 DNA binding domain, fused to the CMV promoter, which was originally shown to act in a dominant negative manner (Ducy et al. 1999). Transfection and selection of clones were performed as already published in details (Bertaux et al. 2006, 2005).

RNA extraction, reverse transcription and polymerase chain reaction (RT–PCR)

Before RNA isolation, MSCs were seeded at 5000 cells/cm^2 and grown for 14 days in osteogenic medium in 25 cm^2 flasks. Selected SaOS-2 clones were seeded in 25 cm^2 flasks at 15,000 cells/cm^2 and cultured in α-MEM for 7 days. Total RNA was extracted using Extract-All reagent according to the manufacturer's instructions. Briefly, lysis of the cells in Extract-All was followed by centrifugation at 12,000 *g* for 15 min, at 4 °C in the presence of chloroform. The upper aqueous phase was collected, and the RNA was precipitated by addition of isopropanol and centrifugation at 12,000 *g* for 10 min, at 4 °C. RNA pellets were washed with 75% ethanol, dried and reconstituted in sterile water. Total RNA was quantified by spectrophotometer at 260 nm wave length and the integrity of RNA was controlled by the 28S/18S rRNA ratio after agarose gel electrophoresis. Contaminating DNA was removed from RNA samples in a 30 min digestion at 37 °C with DNase I. One microgram of each RNA sample was then used for reverse transcription performed under standard conditions with Superscript II reverse transcriptase and random hexamer primers in a 20 μl final volume. The reaction was carried out at 42 °C for 30 min and stopped with incubation at 99 °C for 5 min. The RT reactions were then diluted to 100 μl in water. 1 μl of stock cDNA template was used in subsequent PCR reactions.

Quantitative PCR experiments

Quantitative PCR was performed using a LightCycler system (Roche Diagnostics, Meylan, France) according to the manufacturer's instructions. Reactions were performed in 10 μl volume with 0.3 μM primers, 4 mM $MgCl_2$ and 1 μl of LightCycler-FastStart DNA Master SYBR Green I mix. Protocol consisted of a hot start step (8 min at 95 °C) followed by 40 cycles including a 10 s denaturation step (95 °C), a 10 s annealing step, and an elongation step at 72 °C varying from 15 s to 40 s. The primer sequences and PCR conditions for each cDNA are given in Table 1. Efficiencies of PCR were optimized according to Roche Diagnostic's recommendations on a standard sample expressing all studied genes. To confirm amplification specificity, PCR products were subjected to a melting curve analysis and subsequent gel electrophoresis. Quantification data represented the mean of duplicate conditions. Relative quantification analyses were performed by RelQuant 1.01 Software (Roche Diagnostics, Meylan, France).

Table 1
Summary of primers used.

cDNA	Forward and reverse primers	Ta (°C)	Product (bp)	Genbank
18S	F: 5′-ATTCCGATAACGAACGAGAC-3′ R: 5′-GCTTATGACCCGCACTTACT-3′	62	297	X03205
RPLP0	F: 5′-CGACCTGGAAGTCCAACTAC-3′ R: 5′-AGCAACATGTCCCTGATCTC-3′	60	289	M17885
RUNX2	F: 5′-GCTGTTATGAAAAACCAAGT-3′ R: 5′-GGGAGGATTTGTGAAGAC-3′	60	108	NM_001024630
OC	F: 5′-ATGAGAGCCCTCACACTCCTC-3′ R: 5′-GCCGTAGAAGCGCCGATAGGC-3′	57	293	NM_199173
COL1A2	F: 5′-GGACACAATGGATTGCAAGG-3′ F: 5′-TAACCACTGCTCCACTCTGG-3′	58	461	NM_000089
GAPDH	F: 5′-GTTCCAATATGATTCCACCC-3′ F: 5′-AGGGATGATGTTCTGGAGAG-3′	55	487	M33197

Shown are the primer sequences, annealing temperatures (Ta), lengths of the corresponding PCR products, and Genbank accession numbers of the DNA sequences. F: forward; R: reverse; GAPDH: glyceraldehyde-3-phopshate dehydrogenase; OC: osteocalcin; RPLP0: acidic ribosomal phosphoprotein P0.

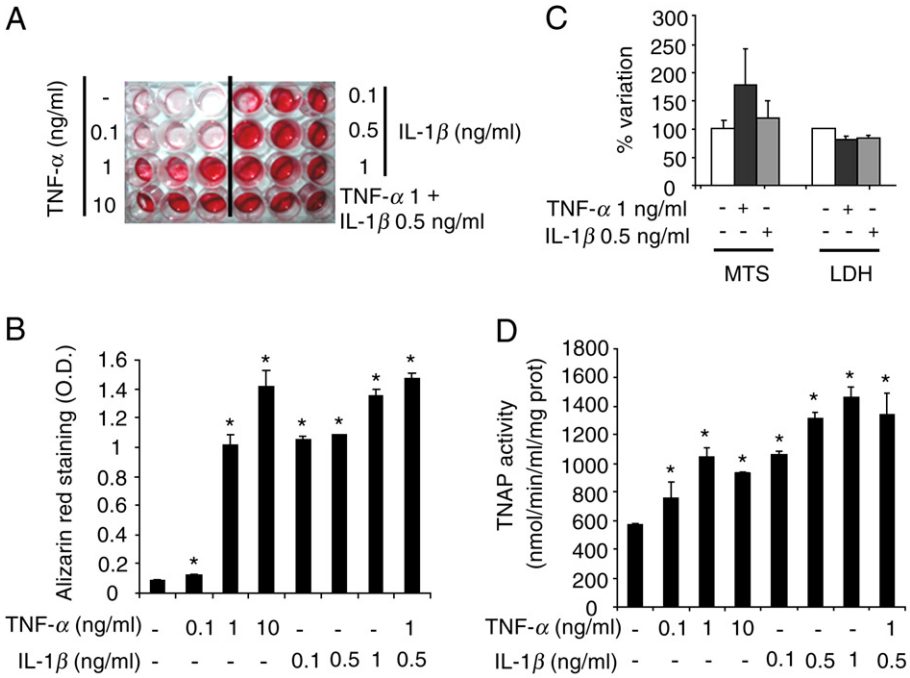

Fig. 1. Dose-dependent effect of TNF-α (0.1 to 10 ng/ml) and IL-1β (0.1 to 1 ng/ml) on alizarin red staining of calcium accumulation (A) in MSCs cultured in 14 days in triplicate conditions in osteogenic medium. (B) Quantification of alizarin red staining in cultures detailed in (A), as described in the "materials and methods" section. (C) Effect of 1 ng/ml of TNF-α or 0.5 ng/ml of IL-1β on cell viability (MTS assay) and death (LDH asay) in MSCs cultured in 14 days in osteogenic medium. (D) Dose-dependent effect of TNF-α (0.1 to 10 ng/ml) and IL-1β (0.1 to 1 ng/ml) on TNAP activity as measured by the method of Lowry in MSCs cultured in 14 days in osteogenic medium. *$P<0.05$ versus control.

TNAP activity

For determination of TNAP activity, MSCs were seeded in 6-well plates at 5000 cells/cm^2 and cultured in osteogenic medium for 14 days. Selected SaOS-2 clones were seeded in 6-well plates at 15,000 cells/cm^2 and cultured in α-MEM for 7 days. MSCs or SaOS-2 cells were harvested in 0.2% Nonidet P-40 and disrupted by sonication. The homogenate was centrifuged at 1500 *g* for 5 min, and TNAP activity in the supernatant was determined by the method of Lowry by measuring the optical density at 405 nm. In the same lysates, the protein content was determined with an assay from BioRad. Results are shown as nmol para-nitrophenol (pNP)/min/mg protein.

Analytical methods

To evaluate cell viability, we used the Cell Titer 96 Aqueus Non-Radioactive Cell Proliferation Assay from Promega (Charbonnières, France), where the formation of formazan from methyltetrazolium salt (MTS) in living adherent cells is quantified by colorimetric measurement at 490 nm. To quantify cell death, we used the lactate dehydrogenase (LDH) assay from Roche (Meylan, France) which measures LDH activity released in culture medium by dead cells. Cells were seeded at 5000 cells/cm^2 in 24-well plates and grown for 7 or 14 days in osteogenic medium before measurement of cell viability or death.

In cells cultured in the same conditions for 14 days, secretion of osteocalcin and RANKL was quantified respectively with Metra Osteocalcin assay from Osteomedical (Paris, France) and with Ampli sRANKL human ELISA from Biomedica (Boldon, England), according to the manufacturer's instructions. Calcium deposition in cell layers was investigated with Alizarin Red staining. Media were discarded and cells were rinsed and stained with 1 ml per well 2% Alizarin Red at pH 4.2 for 2 min and thoroughly washed with water and ethanol 70%. Alizarin red staining was quantified as previously described (Caverzasio et al. 2007). Briefly, mineralization was quantified by extracting the alizarin red stain with 100 mM cetylpyridinium chloride (Sigma-Aldrich) at room temperature for 2 h. Absorbance of the extracted alizarin red stain was measured at 570 nm.

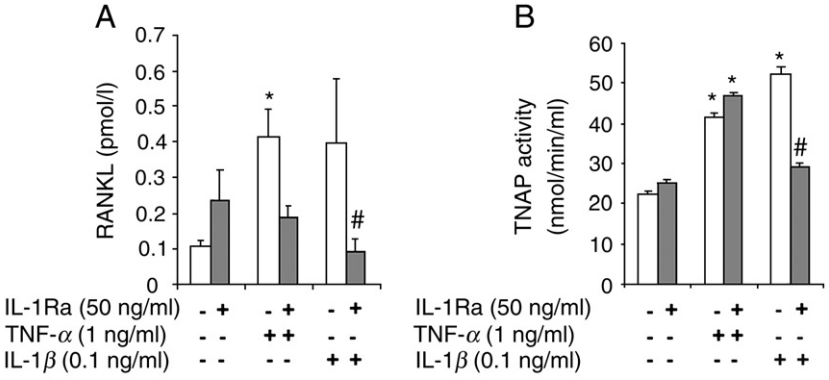

Fig. 2. Effect of 50 ng/ml of IL-1Ra on RANKL levels (A, measured by ELISA) and TNAP activity (B, measured by the method of Lowry) in MSCs cultured in 14 days in osteogenic medium, in presence or absence of 1 ng/ml of TNF-α or 0.5 ng/ml of IL-1β, as detailed in the "materials and methods" section. *$P<0.05$ versus control; #$P<0.05$ versus IL-1β-treated cells.

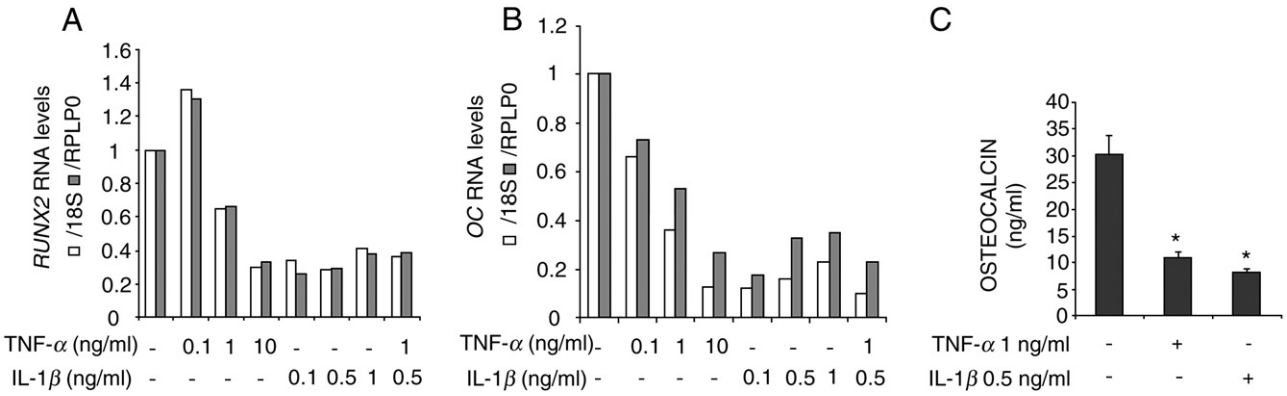

Fig. 3. Dose-dependent effect of TNF-α (0.1 to 10 ng/ml) and IL-1β (0.1 to 1 ng/ml) on *RUNX2* (A) and *OC* (B) RNA levels in MSCs cultured in 14 days in osteogenic medium, as determined by real-time PCR, after correction for 18S (empty bars) or RPLP0 (full bars) RNA levels. (C) Effect of 1 ng/ml of TNF-α or 0.5 ng/ml of IL-1β on OC secretion (measured by ELISA) in MSCs cultured in 14 days in osteogenic medium. *$P<0.05$ versus control. RPLP0: acidic ribosomal phosphoprotein P0.

Statistical analysis

All experiments were performed in triplicates and repeated at least twice. Similar results were obtained from the four cell types used in the present study. Because results were obtained with MSCs in stromal cells (three patients) and with purified MSCs (one donor), data were not pooled and results of one representative experiment are shown. Results are expressed as mean ± the standard error of the mean (SEM). For statistical analysis, a Mann–Whitney test was used. A difference between experimental groups was considered to be significant when $P<0.05$.

Results

In a previous study (Isaac et al. 2008), we observed that when MSCs were cultured in an osteogenic medium, a red staining was already noticeable after 14 days, whereas cells cultured in control conditions remained unstained. In the present study, to investigate the effects of cytokines on mineralization, cells were therefore cultured for 14 days in osteogenic medium in presence of 0.1 to 10 ng/ml TNF-α, 0.1 to 1 ng/ml IL-1β, or a combination of both cytokines.

First, in cultures in osteogenic medium without cytokines, a red staining was noticeable on day 14 confirming our previous studies with the same cells (Isaac et al. 2008). In addition, we surprisingly but consistently observed a dose-dependent positive effect of TNF-α and IL-1β on calcium accumulation, with a more potent effect of IL-1β than TNF-α (Fig. 1A and B). Because TNF-α has been reported to promote cell death in osteoblast culture (Hill et al. 1997), we suspected that calcium accumulation in presence of cytokines may have been due to the physico-chemical precipitation that is commonly observed during cell death in bone cell cultures (Magne et al. 2003). However, measurement of cell death and viability after 14 days in culture, with LDH and MTS assays, indicated that the cytokines did not even slightly reduce cell viability or induce cell death respectively (Fig. 1C). This was confirmed by cell counts after 7 and 14 days in either growth medium or osteogenic medium, which did not reveal any antiproliferative effects of either cytokine (data not shown). Therefore, the stimulation of alizarin red staining by TNF-α and IL-1β could not be related to differences in cell number or viability. We then aimed at determining the mechanisms responsible for this increase in mineralization, taking into account that cell-mediated mineralization may merely depend on an increase in alkaline phosphatase activity in a tissue containing a fibrillar collagen (Murshed et al. 2005). Measurement of TNAP activity showed a significant increase upon treatment with increasing doses of TNF-α or IL-1β (Fig. 1D), suggesting that the positive effects of cytokines on mineralization were due to stimulation in TNAP activity.

We next questioned whether TNF-α effects on TNAP activity were due to IL-1 signaling, as it is the case in bone marrow stromal cells for TNF-α-induced RANKL expression (Wei et al. 2005). Indeed, Wei et al. demonstrated that TNF-α stimulated the expression of the IL-1 receptor, which was responsible for RANKL secretion, because the TNF-α effects were blocked by IL-1Ra (Wei et al. 2005). In our study, cells were co-treated for 14 days with 50 ng/ml of IL-1Ra and 1 ng/ml of TNF-α or 0.1 ng/ml of IL-1β in culture medium. In our experiments, IL-1Ra seemed to decrease RANKL secretion in response to TNF-α, although this was not significant, probably because of the variability in RANKL levels (Fig. 2A). Nevertheless, IL-1Ra never decreased, even slightly, TNAP activity in response to TNF-α whereas it abolished the stimulatory effect of IL-1β (Fig. 2B). These results clearly indicate that IL-1 is unnecessary for TNF-α effects on TNAP activity.

We next aimed at investigating whether or not cytokine positive effects on TNAP activity and mineralization were accompanied by a

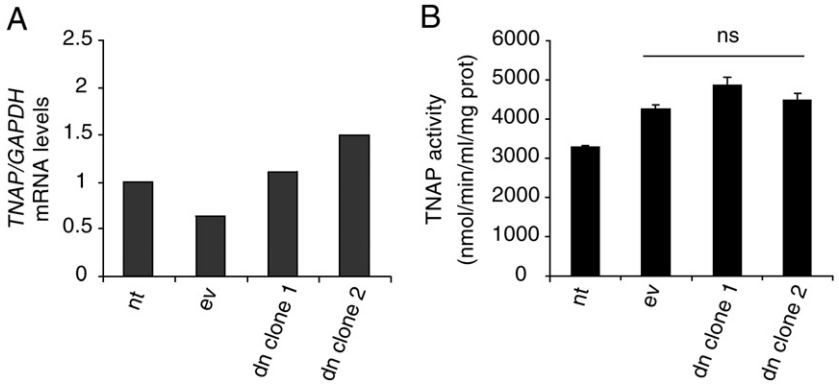

Fig. 4. *TNAP* RNA levels (A) and TNAP activity (B) in nontransfected (nt) SaOS-2 cells, and in SaOS-2 clones transfected either with empty vector (ev) or with RUNX2 dominant negative (dn) construct. Cells were cultured for 7 days and RNA levels and enzyme activity were measured by quantitative PCR and the method of Lowry respectively. ns: not significant.

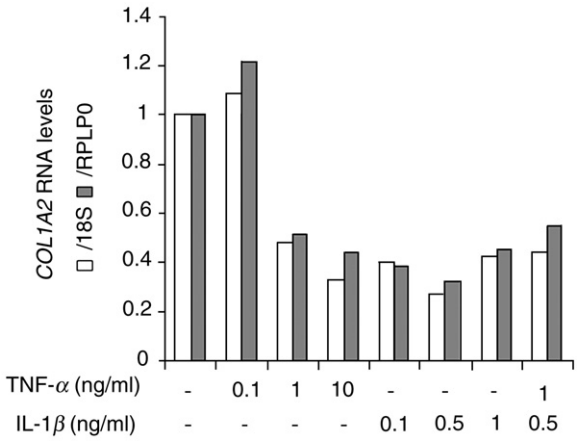

Fig. 5. Dose-dependent effect of TNF-α (0.1 to 10 ng/ml) and IL-1β (0.1 to 1 ng/ml) on *COL1A2* RNA levels in MSCs cultured in 14 days in osteogenic medium, as determined by real-time PCR, after correction for 18S (empty bars) or RPLP0 (full bars) RNA levels. RPLP0: acidic ribosomal phosphoprotein P0.

stimulation of osteoblast differentiation from MSCs. To this purpose, we analyzed the expression pattern of RUNX2, the master transcription factor in osteoblast differentiation. Fig. 3A clearly indicates that both cytokines decreased *RUNX2* RNA levels, with a much more pronounced effect of IL-1β (from 0.1 ng/ml), as compared to TNF-α (at 10 ng/ml). This decrease in *RUNX2* RNA levels was likely accompanied by a drop in RUNX2 activity, because RNA and protein levels of one of its transcriptional targets, *OC*, mimicked RUNX2 expression (Fig. 3B and C).

Cytokine effects on TNAP activity and mineralization therefore appear independent upon RUNX2 activity in human MSCs. To confirm this hypothesis, dominant negative RUNX2 was overexpressed in human osteoblast-like cells and clones were obtained as previously published in details (Bertaux et al. 2006, 2005). Quantitative PCR results shown in Fig. 4A indicate that expression of *TNAP* was not reduced in absence of functional RUNX2. Moreover, TNAP activity was identical in clones transfected with dominant negative RUNX2 or with empty vector (Fig. 4B), further suggesting that RUNX2 is not involved in TNAP expression in osteoblasts.

Finally, because cytokines do not decrease TNAP activity in osteoblasts, we hypothesized that their reported negative effect on bone formation is due to decreased secretion of collagen fibrils, which serve as a template for crystal deposition and multiplication. Quantitative PCR experiments showed that upon treatment with TNF-α and IL-1β, the expression pattern of *COL1A2* was very similar to that of *RUNX2*, with a dose-dependent negative effect of TNF-α and a more robust inhibitory effect of IL-1β (Fig. 5). Together with our recently published finding that expression of *COL1A2* depends on RUNX2 (Bertaux et al. 2006), this result strongly suggests that cytokines decrease type I collagen expression by inhibiting RUNX2.

Discussion

Our results indicate that TNF-α and IL-1β decrease *RUNX2* levels in osteoblasts differentiated from human MSCs. This is in accordance with previous studies in mouse cells indicating that TNF-α decreases *RUNX2* expression (Gilbert et al. 2002) and promotes its degradation (Kaneki et al. 2006). Inhibition of RUNX2 activity appears also confirmed in our study by decreased expression of *COL1A2* and *OC*, which are dependent on RUNX2 activity (Ducy et al. 1997).

However and in contrast to these data, other findings have reported a positive effect of TNF-α on RUNX2 and/or OC in VSMCs, myofibroblasts and interstitial cells (Kaden et al. 2005; Tintut et al. 2000). Although cell-specific differences in the response to cytokines cannot be excluded, we speculate that RUNX2 stimulation in these studies was not a direct effect of cytokines, but was rather a result of induction of TNAP activity and mineralization. In this hypothesis, RUNX2 expression and osteoblast differentiation may be induced when cells grow on a calcified matrix. Several reports support this model. Firstly, inhibition of TNAP activity with levamisole was shown to inhibit expression of osteogenic markers in interstitial cells (Mathieu et al. 2005). Secondly, TNAP small interfering (si) RNA dramatically reduced osteocalcin expression in osteoblasts (Kotobuki et al. 2008). This model is coherent with recently published data on vascular calcification, occurring during atherosclerosis or type II diabetes. Indeed, intravital imaging studies with *ApoE*-/- mice on a high fat diet showed that in early-stage atherosclerosis, presence of macrophages preceded calcification, suggesting that macrophages sent specific inflammatory signals to vascular wall cells to initiate calcification (Aikawa et al. 2007). Interestingly, TNAP activity in VSMC was stimulated by conditioned media from macrophages, but significantly less in presence of anti-TNF-α antibodies (Shioi et al. 2002; Tintut et al. 2002). The same pattern may be true in type II diabetes, since in *ldlr*-/- diabetic mice, treatment with the TNF-α inhibitor infliximab specifically reduced inflammation and aortic calcification, but not *RUNX2* expression (Al-Aly et al. 2007). This suggests that TNF-α does not directly stimulate RUNX2, in contrast to TNAP activity and calcification.

The most interesting finding in our study may be that although both TNF-α and IL-1β strongly inhibited RUNX2, they were able to stimulate TNAP activity and mineralization. Actually, TNAP activity and mineralization do not always mirror RUNX2 activity. In tibiae from *RUNX2*-deficient embryos for instance, perichondrial cells expressed *TNAP* (Hoshi et al. 1999). The inability of these cells to calcify their matrix was likely due to lack of type I collagen secretion (Hoshi et al. 1999). Indeed, formation of a calcified tissue requires the presence of a fibrillar collagen, as a template for crystal deposition, and an increase in TNAP activity to remove pyrophosphate ions (PPi), which are powerful mineralization inhibitors (Murshed et al. 2005). This model seems validated by the fact that calcified cartilage developed in the tibiae of *RUNX2*-deficient embryos (Komori et al. 1997; Otto et al. 1997), likely because cartilage contains type II collagen, which is dependent on sox9 (Bell et al. 1997) and independent from RUNX2 activity. Moreover, these in vivo data confirm findings from several in vitro studies. For instance, in human osteoblast-like cells, inhibition of RUNX2 expression with siRNA did not decrease TNAP activity (Kotobuki et al. 2008), and in our study, overexpression of a dominant negative RUNX2 did not decrease TNAP activity either, confirming that TNAP expression is unrelated to RUNX2. RUNX2 therefore appears to display two functions in relation with bone formation: osteoblast differentiation during development and matrix deposition by differentiated osteoblasts in the adulthood (Ducy et al. 1999).

The cytokine inhibitory effect on RUNX2 and positive action on TNAP activity may help explain the different patterns of bone remodeling observed in RA and in SpAs. In RA, the fact that bone formation does not compensate for resorption may be explained by cytokine inhibition of RUNX2-dependent collagen synthesis. In contrast, in SpAs, new bone formation at the sites of enthesopathic peripheral joint and spine inflammation often accompanies marked osteopenia of the spinal column itself (Walsh et al. 2005). This new bone formation may be due to inflammatory cytokines, since in patients with ankylosing spondylitis, new bone formation occurs significantly more often in vertebral edges with than without spinal inflammation (Baraliakos et al. 2008), and since entheseal osteitis is reduced by anti-TNF treatment (Marzo-Ortega et al. 2005). As mineralization only requires the coexpression of TNAP and collagen (Murshed et al. 2005), our results showing that inflammatory cytokines increase TNAP activity suggest that in SpAs, calcification of collagen-rich entheses may be initiated by the mere removal of the mineralization inhibitor PPi by increased TNAP action.

Conclusion

In conclusion, our experiments reveal that in cultured human MSCs, the major inflammatory cytokines TNF-α and IL-1β inhibit collagen expression while they stimulate TNAP activity. If confirmed in vivo, these data may help understand the different impact of inflammation on normal and ectopic bone formation. This hypothesis is today under intense investigation.

Acknowledgements

This study was supported by the INSERM French National Program for Osteoarticular Diseases (PRO-A). Authors also thank Dr. C. Morin (Service d'Orthopédie Pédiatrique, Institut Calot Berck, France) for providing tissue samples.

References

Aikawa E, Nahrendorf M, Figueiredo JL, Swirski FK, Shtatland T, Kohler RH, Jaffer FA, Aikawa M, Weissleder R. Osteogenesis associates with inflammation in early-stage atherosclerosis evaluated by molecular imaging in vivo. Circulation 116 (24), 2841–2850, 2007.

Al-Aly Z, Shao JS, Lai CF, Huang E, Cai J, Behrmann A, Cheng SL, Towler DA. Aortic Msx2-Wnt calcification cascade is regulated by TNF-alpha-dependent signals in diabetic Ldlr-/- mice. Arteriosclerosis, Thrombosis, and Vascular Biology 27 (12), 2589–2596, 2007.

Ammann P, Rizzoli R, Bonjour JP, Bourrin S, Meyer JM, Vassalli P, Garcia I. Transgenic mice expressing soluble tumor necrosis factor-receptor are protected against bone loss caused by estrogen deficiency. Journal of Clinical Investigation 99 (7), 1699–1703, 1997.

Anselme K, Noel B, Limosino D, Bianchi F, Morin C, Hardouin P. Comparative study of the in vitro characteristics of osteoblasts from paralytic and non-paralytic children. Spinal Cord 38 (10), 622–629, 2000.

Baraliakos X, Listing J, Rudwaleit M, Brandt J, Sieper J, Braun J. Evidence for a link between inflammation and new bone formation in ankylosing spondylitis. In: Dis, A.R. (Ed.), 28th European Workshop for Rheumatology, p. A39. Toulouse.

Bell DM, Leung KK, Wheatley SC, Ng LJ, Zhou S, Ling KW, Sham MH, Koopman P, Tam PP, Cheah KS. SOX9 directly regulates the type-II collagen gene. Nature Genetics 16 (2), 174–178, 1997.

Bertaux K, Broux O, Chauveau C, Jeanfils J, Devedjian JC. Identification of CBFA1-regulated genes on SaOs-2 cells. Journal of Bone and Mineral Metabolism 23 (2), 114–122, 2005.

Bertaux K, Broux O, Chauveau C, Hardouin P, Jeanfils J, Devedjian JC. Runx2 regulates the expression of GNAS on SaOs-2 cells. Bone 38 (6), 943–950, 2006.

Caverzasio J, Manen D. Essential role of Wnt3a-mediated activation of mitogen-activated protein kinase p38 for the stimulation of alkaline phosphatase activity and matrix mineralization in C3H10T1/2 mesenchymal cells. Endocrinology 148 (11), 5323–5330, 2007.

Charatcharoenwitthaya N, Khosla S, Atkinson EJ, McCready LK, Riggs BL. Effect of blockade of TNF-alpha and interleukin-1 action on bone resorption in early postmenopausal women. Journal of Bone and Mineral Research 22 (5), 724–729, 2007.

Demer LL. Vascular calcification and osteoporosis: inflammatory responses to oxidized lipids. International Journal of Epidemiology 31 (4), 737–741, 2002.

Doherty TM, Asotra K, Fitzpatrick LA, Qiao JH, Wilkin DJ, Detrano RC, Dunstan CR, Shah PK, Rajavashisth TB. Calcification in atherosclerosis: bone biology and chronic inflammation at the arterial crossroads. Proceedings of the National Academy of Sciences of the United States of America 100 (20), 11201–11206, 2003.

Ducy P, Zhang R, Geoffroy V, Ridall AL, Karsenty G. Osf2/Cbfa1: a transcriptional activator of osteoblast differentiation. Cell 89 (5), 747–754, 1997.

Ducy P, Starbuck M, Priemel M, Shen J, Pinero G, Geoffroy V, Amling M, Karsenty G. A Cbfa1-dependent genetic pathway controls bone formation beyond embryonic development. Genes & Development 13 (8), 1025–1036, 1999.

Gilbert L, He X, Farmer P, Rubin J, Drissi H, van Wijnen AJ, Lian JB, Stein GS, Nanes MS. Expression of the osteoblast differentiation factor RUNX2 (Cbfa1/AML3/Pebp2alpha A) is inhibited by tumor necrosis factor-alpha. Journal of Biological Chemistry 277 (4), 2695–2701, 2002.

Helske S, Kupari M, Lindstedt KA, Kovanen PT. Aortic valve stenosis: an active atheroinflammatory process. Current Opinion in Lipidology 18 (5), 483–491, 2007.

Hill PA, Tumber A, Meikle MC. Multiple extracellular signals promote osteoblast survival and apoptosis. Endocrinology 138 (9), 3849–3858, 1997.

Hoshi K, Komori T, Ozawa H. Morphological characterization of skeletal cells in Cbfa1-deficient mice. Bone 25 (6), 639–651, 1999.

Isaac J, Hornez JC, Jian D, Descamps M, Hardouin P, Magne D. Beta-TCP microporosity decreases the viability and osteoblast differentiation of human bone marrow stromal cells. Journal of Biomedical Materials Research A 86 (2), 386–393, 2008.

Jimi E, Nakamura I, Duong LT, Ikebe T, Takahashi N, Rodan GA, Suda T. Interleukin 1 induces multinucleation and bone-resorbing activity of osteoclasts in the absence of osteoblasts/stromal cells. Experimental Cell Research 247 (1), 84–93, 1999.

Kaden JJ, Kilic R, Sarikoc A, Hagl S, Lang S, Hoffmann U, Brueckmann M, Borggrefe M. Tumor necrosis factor alpha promotes an osteoblast-like phenotype in human aortic valve myofibroblasts: a potential regulatory mechanism of valvular calcification. International Journal of Molecular Medicine 16 (5), 869–872, 2005.

Kaneki H, Guo R, Chen D, Yao Z, Schwarz EM, Zhang YE, Boyce BF, Xing L. Tumor necrosis factor promotes Runx2 degradation through up-regulation of Smurf1 and Smurf2 in osteoblasts. Journal of Biological Chemistry 281 (7), 4326–4333, 2006.

Kimble RB, Matayoshi AB, Vannice JL, Kung VT, Williams C, Pacifici R. Simultaneous block of interleukin-1 and tumor necrosis factor is required to completely prevent bone loss in the early postovariectomy period. Endocrinology 136 (7), 3054–3061, 1995.

Kimble RB, Bain S, Pacifici R. The functional block of TNF but not of IL-6 prevents bone loss in ovariectomized mice. Journal of Bone and Mineral Research 12 (6), 935–941, 1997.

Kitaura H, Sands MS, Aya K, Zhou P, Hirayama T, Uthgenannt B, Wei S, Takeshita S, Novack DV, Silva MJ, Abu-Amer Y, Ross FP, Teitelbaum SL. Marrow stromal cells and osteoclast precursors differentially contribute to TNF-alpha-induced osteoclastogenesis in vivo. Journal of Immunology 173 (8), 4838–4846, 2004.

Kitaura H, Zhou P, Kim HJ, Novack DV, Ross FP, Teitelbaum SL. M-CSF mediates TNF-induced inflammatory osteolysis. Journal of Clinical Investigation 115 (12), 3418–3427, 2005.

Kitazawa R, Kimble RB, Vannice JL, Kung VT, Pacifici R. Interleukin-1 receptor antagonist and tumor necrosis factor binding protein decrease osteoclast formation and bone resorption in ovariectomized mice. Journal of Clinical Investigation 94 (6), 2397–2406, 1994.

Komori T, Yagi H, Nomura S, Yamaguchi A, Sasaki K, Deguchi K, Shimizu Y, Bronson RT, Gao YH, Inada M, Sato M, Okamoto R, Kitamura Y, Yoshiki S, Kishimoto T. Targeted disruption of Cbfa1 results in a complete lack of bone formation owing to maturational arrest of osteoblasts. Cell 89 (5), 755–764, 1997.

Kotobuki N, Matsushima A, Kato Y, Kubo Y, Hirose M, Ohgushi H. Small interfering RNA of alkaline phosphatase inhibits matrix mineralization. Cell and Tissue Research 332 (2), 279–288, 2008.

Lorenzo JA, Naprta A, Rao Y, Alander C, Glaccum M, Widmer M, Gronowicz G, Kalinowski J, Pilbeam CC. Mice lacking the type I interleukin-1 receptor do not lose bone mass after ovariectomy. Endocrinology 139 (6), 3022–3025, 1998.

Magne D, Bluteau G, Faucheux C, Palmer G, Vignes-Colombeix C, Pilet P, Rouillon T, Caverzasio J, Weiss P, Daculsi G, Guicheux J. Phosphate is a specific signal for ATDC5 chondrocyte maturation and apoptosis-associated mineralization: possible implication of apoptosis in the regulation of endochondral ossification. Journal of Bone and Mineral Research 18 (8), 1430–1442, 2003.

Magne D, Julien M, Vinatier C, Merhi-Soussi F, Weiss P, Guicheux J. Cartilage formation in growth plate and arteries: from physiology to pathology. Bioessays 27 (7), 708–716, 2005.

Marzo-Ortega H, McGonagle D, Jarrett S, Haugeberg G, Hensor E, O'Connor P, Tan AL, Conaghan PG, Greenstein A, Emery P. Infliximab in combination with methotrexate in active ankylosing spondylitis: a clinical and imaging study. Annals of Rheumatic Diseases 64 (11), 1568–1575, 2005.

Mathieu P, Voisine P, Pepin A, Shetty R, Savard N, Dagenais F. Calcification of human valve interstitial cells is dependent on alkaline phosphatase activity. Journal of Heart Valve Disease 14 (3), 353–357, 2005.

Murshed M, Harmey D, Millan JL, McKee MD, Karsenty G. Unique coexpression in osteoblasts of broadly expressed genes accounts for the spatial restriction of ECM mineralization to bone. Genes & Development 19 (9), 1093–1104, 2005.

Otto F, Thornell AP, Crompton T, Denzel A, Gilmour KC, Rosewell IR, Stamp GW, Beddington RS, Mundlos S, Olsen BR, Selby PB, Owen MJ. Cbfa1, a candidate gene for cleidocranial dysplasia syndrome, is essential for osteoblast differentiation and bone development. Cell 89 (5), 765–771, 1997.

Parhami F, Basseri B, Hwang J, Tintut Y, Demer LL. High-density lipoprotein regulates calcification of vascular cells. Circulation Research 91 (7), 570–576, 2002.

Shao JS, Cai J, Towler DA. Molecular mechanisms of vascular calcification: lessons learned from the aorta. Arteriosclerosis, Thrombosis, and Vascular Biology 26 (7), 1423–1430, 2006.

Shioi A, Katagi M, Okuno Y, Mori K, Jono S, Koyama H, Nishizawa Y. Induction of bone-type alkaline phosphatase in human vascular smooth muscle cells: roles of tumor necrosis factor-alpha and oncostatin M derived from macrophages. Circulation Research 91 (1), 9–16, 2002.

Tintut Y, Patel J, Parhami F, Demer LL. Tumor necrosis factor-alpha promotes in vitro calcification of vascular cells via the cAMP pathway. Circulation 102 (21), 2636–2642, 2000.

Tintut Y, Patel J, Territo M, Saini T, Parhami F, Demer LL. Monocyte/macrophage regulation of vascular calcification in vitro. Circulation 105 (5), 650–655, 2002.

Walsh NC, Crotti TN, Goldring SR, Gravallese EM. Rheumatic diseases: the effects of inflammation on bone. Immunological Reviews 208, 228–251, 2005.

Wei S, Kitaura H, Zhou P, Ross FP, Teitelbaum SL. IL-1 mediates TNF-induced osteoclastogenesis. Journal of Clinical Investigation 115 (2), 282–290, 2005.